76 SPATIAL MAPPING OF T CELL RECEPTORS AND TRANSCRIPTOMES IN RENAL CELL CARCINOMA FOLLOWING IMMUNE CHECKPOINT INHIBITOR THERAPY

[1]Sophia Liu, [2]Bryan Iorgulescu*, [3]Shuqiang Li, [1]Julia Morriss, [3]Mehdi Borji, [1]Evan Murray, [3]David Braun, [3]Kenneth Livak, [3]Catherine Wu, [1]Fei Chen. [1]*Broad Institute, Cambridge, USA*; [2]*Dana-Farber Cancer Institute, Boston, MA, USA*; [3]*DFCI, Cambridge, MA, USA*

Background Because conventional single-cell strategies rely on dissociating tissues into suspensions that lose spatial context,[1] we developed Slide-TCR-seq to sequence both whole transcriptomes and TCRs with 10μm-spatial resolution, & applied it to renal cell carcinoma (ccRCC) treated with immune checkpoint inhibitors (ICI).

Methods Slide-TCR-seq combines Slide-seqV2[2] [3]—a 10μm-resolution spatial approach utilizing mRNA capture and DNA-barcoded beads—with sensitive targeted capture of TCR sequences (rhTCRseq,[4] previously developed by our group), thereby enabling amplification of segments extending from upstream of CDR3 to the 3'-end of the TCR transcript (figure 1A). We tested Slide-TCR-seq first on OT-I murine spleen and then applied this methodology to 3 patients' pre-αPD-1 ccRCC samples[5] and a post-αPD-1 metastasis to investigate the spatial, functional, and clonotypic organization of T cells in relationship to tumor using RCTD,[6] spatial enrichment, and spatial expression analyses.

Results Using Slide-TCR-seq, we first recapitulated native spatial structure of OT-I mouse spleen (figure 1B-G). TCR□/β CDR3 sequences were detected on 37.1% of beads with Trac/Trbc2 constant sequences—comparable to other scTCRseq methods. Because the clonal and spatial context of TILs have been increasingly implicated in immunotherapy resistance, we used Slide-TCR-seq to analyze a lung ccRCC metastasis following αPD-1 therapy. We employed unsupervised clustering to delineate the tumor, intervening boundary, and lung compartments, and RCTD analyses to spatially map individual cell types; together recapitulating the architecture observed in corresponding histology (figure 2). We identified 1,132 unique clonotypes, with distinct spatial distributions spanning the tissue compartments. Eight clonotypes were significantly enriched in tumor, whereas 5 were depleted (all $p<0.05$) (figure 3). We then analyzed the relationships between the T cells' clonotype, gene expression, and tumor infiltration depth among clonotypes. Using a T-cell geneset associated with poor response to ICI,[7] we dichotomized T-clonotype beads by geneset expression, and found spatial segregation of this geneset's expression both within and across clonotypes (figure 4). TCR-4—the most significantly tumor-enriched clonotype—and TCR-2 displayed high expression of the poor ICI response geneset near the tumor's edge, but low expression deeper in the tumor compartment; indicating that there are transcriptionally distinct subpopulations of these clonotypes, which depended on the extent of their tumor infiltration.

Conclusions Slide-TCR-seq effectively integrates spatial transcriptomics with TCR detection at 10μm resolution, thereby relating T cells' clonality and gene expression to their spatial organization in tumors. Our findings suggest that a clonotype's T cells may exhibit mixed responses to ICI depending on their spatial localization. The heterogeneity among clonotypes, in both gene expression and organization, underscores the importance of studying the TCR repertoire with spatial resolution.

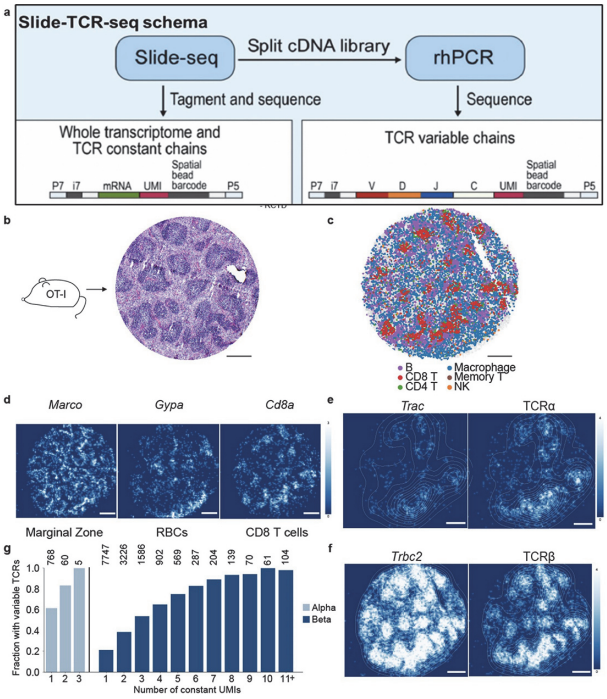

Abstract 76 Figure 1 Slide-TCR-seq spatially localizes T cell receptors and transcriptome information. a. Schematic of Slide-TCR-seq, in which tissue is placed onto an in situ barcoded bead array. cDNA libraries prepared with Slide-seqV2 are split prior to fragmentation with one portion used for targeted amplification via rhTCRseq optimized for use with Slide-seq libraries. Slide-TCR-seq provides gene expression, cell type, and clonotype information in space. b. Serial sections of the OT-1 mouse spleen with hematoxylin and eosin stain show characteristic architecture of red pulp and white pulp separation. c. Spatial reconstruction of Slide-TCR-seq array for a corresponding section of OT-I mouse spleen, with RCTD immune cell type assignment. NK = natural killer. d. Gene expression gaussian-filtered heatmap for visualizing the spatial distribution of gene markers for marginal zone (Marco), red blood cells (RBCs; Gypa), and CD8 T cells (Cd8a). e and f. Comparing the spatial distribution of constant (left) and variable (right) sequences for TCRα (e) and TCRβ (f), with superimposed density plot. g. The fraction of beads that capture CDR3 variable sequences (y-axis) when constant UMIs are captured (x-axis) for TCRα (left, light blue) and TCRβ (right, dark blue), with the number of corresponding beads along the top axis. All scale bars: 500 μm.

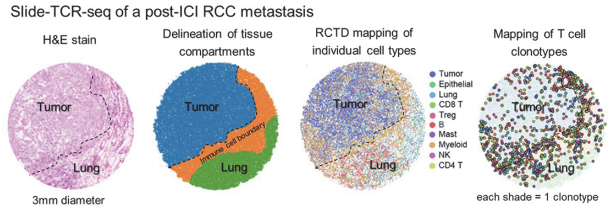

Abstract 76 Figure 2 Slide-TCR-seq identifies spatial differences between T cell clonotypes in renal cell carcinoma. (a) H&E stain of a ccRCC metastasis to the lung following PD-1 blockade therapy. (b) The compartment assignment of lung (green), immune cell boundary (orange), and tumor (blue) by applying K-nearest neighbors to cell types determined by unsupervised clustering from Slide-TCR-seq of a sequential tissue section. (c) Spatial reconstruction of cell type identifies using RCTD anaysis of the Slide-TCR-seq data. (d) Spatial localization of T cell clonotypes (n=447 clonotypes, colored by clonotype) from the the Slide-TCR-seq data.

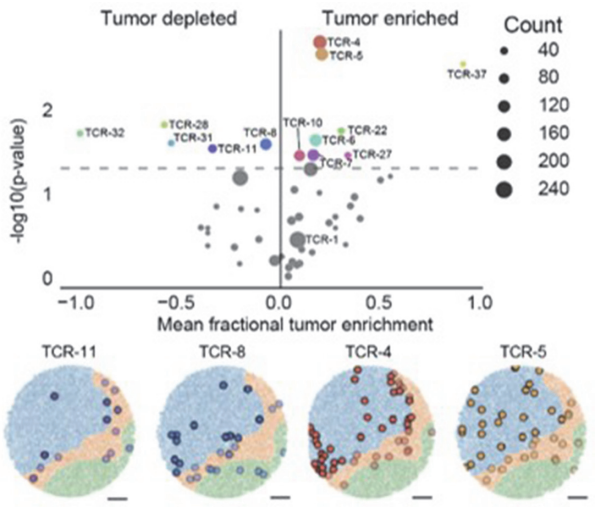

Abstract 76 Figure 3 Top: y-axis Significance of clonotype spatial distributions compared against all other clonotypes with at least ten beads per array from the ccRCC lung metastasis plotted against an x-axis of magnitude of tumor enrichment or depletion (data from n=3 replicate arrays, two one-tailed K-S tests). Bottom: Visualization of selected significant clonotypes, ordered by tumor enrichment, in tissue compartments for a single array (T cells within the tumor compartment are displayed as opaque, T cells within other compartments are displayed as translucent).

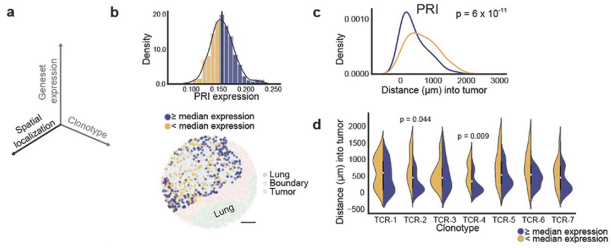

Abstract 76 Figure 4 Spatial and molecular heterogeneity in clonotype gene expression and tumor infiltration. a. The three axes — spatial localization, gene expression, and T cell clonotype — that Slide-TCR-seq can relate. b. Top: distribution of poor response to immune checkpoint inhibitor treatment ('PRI') geneset[7] expression across all clonotypes in the tumor region of the same post-PD1 inhibitor RCC lung metastasis from figures 2–3 (from a single replicate) with kernel density estimation. Yellow = clonotypes with lower than median PRI expression; purple = clonotypes with PRI expression greater than or equal to the median value. Bottom: localization of low (yellow) and high (purple) PRI geneset expression clonotypes within the tumor region (light blue) from the Slide-TCR-seq array shows their distinct spatial separation (light blue = tumor region, orange = boundary region, green = lung region). Scale bar: 500 μm. c. Smoothed histograms comparing the distance infiltrated into tumor by two-tailed K-S test comparing low (yellow) and high (purple) expression clonotypes, as dichotomized by median expression of PRI. d. Comparing distance infiltrated into tumor by two-tailed K-S test between low and high PRI expression T cells across those clonotypes with at least 20 beads (n=7 clonotypes).

Acknowledgements We are grateful to Irving A. Barrera-Lopez, Zoe N. Garcia, and Aziz Al'Khafaji for technical assistance.

REFERENCES

1. Gohil S, Iorgulescu JB, Braun D, Keskin D, Livak K. Applying high-dimensional single-cell technologies to the analysis of cancer immunotherapy. *Nat Rev Clin Oncol* 2021; **18**:244–256.
2. Stickels RR, Murray E, Kumar P, Li J, Marshall JL, Di Bella DJ, Arlotta P, Macosko EZ, Chen F. Highly sensitive spatial transcriptomics at near-cellular resolution with Slide-seqV2. *Nat Biotechnol* 2021 Mar;**39**(3):313–319.
3. Rodriques SG, Stickels RR, Goeva A, Martin CA, Murray E, Vanderburg CR, Welch J, Chen LM, Chen F, Macosko EZ. Slide-seq: A scalable technology for measuring genome-wide expression at high spatial resolution. *Science* 2019 Mar 29;**363** (6434):1463–1467.
4. Li S, Sun J, Allesøe R, Datta K, Bao Y, Oliveira G, Forman J, Jin R, Olsen LR, Keskin DB, Shukla SA, Wu CJ, Livak KJ. RNase H-dependent PCR-enabled T-cell receptor sequencing for highly specific and efficient targeted sequencing of T-cell receptor mRNA for single-cell and repertoire analysis. *Nat Protoc* 2019 Aug;**14** (8):2571–2594.
5. Braun DA, Street K, Burke KP, Cookmeyer DL, Denize T, Pedersen CB, Gohil SH, Schindler N, Pomerance L, Hirsch L, Bakouny Z, Hou Y, Forman J, Huang T, Li S, Cui A, Keskin DB, Steinharter J, Bouchard G, Sun M, Pimenta EM, Xu W, Mahoney KM, McGregor BA, Hirsch MS, Chang SL, Livak KJ, McDermott DF, Shukla SA, Olsen LR, Signoretti S, Sharpe AH, Irizarry RA, Choueiri TK, Wu CJ. Progressive immune dysfunction with advancing disease stage in renal cell carcinoma. *Cancer Cell* 2021 May 10;**39**(5):632–648.
6. Cable DM, Murray E, Zou LS, Goeva A, Macosko EZ, Chen F, Irizarry RA. Robust decomposition of cell type mixtures in spatial transcriptomics. *Nat Biotechnol* 2021 Feb 18. doi: 10.1038/s41587-021-00830-w. Epub ahead of print. PMID: 33603203.
7. Sade-Feldman M, Yizhak K, Bjorgaard SL, Ray JP, de Boer CG, Jenkins RW, Lieb DJ, Chen JH, Frederick DT, Barzily-Rokni M, Freeman SS, Reuben A, Hoover PJ, Villani AC, Ivanova E, Portell A, Lizotte PH, Aref AR, Eliane JP, Hammond MR, Vitzthum H, Blackmon SM, Li B, Gopalakrishnan V, Reddy SM, Cooper ZA, Paweletz CP, Barbie DA, Stemmer-Rachamimov A, Flaherty KT, Wargo JA, Boland GM, Sullivan RJ, Getz G, Hacohen N. Defining T Cell States Associated with Response to Checkpoint Immunotherapy in Melanoma. *Cell* 2018 Nov 1;**175**(4):998–1013

Ethics Approval This study was approved by MGB/DFCI/Broad institution's Ethics Board; approval number 2019P000017.

http://dx.doi.org/10.1136/jitc-2021-SITC2021.076